Rotational excitation of N_2 by electron impact: 1–4 eV

S. F. Wong and L. Dubé
Department of Engineering and Applied Science, Mason Laboratory, Yale University, New Haven, Connecticut 06520
(Received 17 October 1977)

Rotational and rotational-vibrational ($v = 0 \rightarrow 1$) excitation in N_2 have been studied with a crossed-beam electron-impact apparatus. In the energy range 1–4 eV, the elastic and vibrational energy-loss peaks show large rotational broadening compared with the apparatus profile (full width at half-maximum, 18 meV). The branching ratios for rotational transitions with $\Delta j = 0, \pm 2, \pm 4$ are obtained with a line-shape analysis applied to the energy-loss profiles. The results for rotational-vibrational excitation at 2.27 eV and scattering angles 30–90° are in good agreement with the calculations using the resonant $d\pi$ waves and the rotational impulse approximation. The corresponding results for pure rotational excitation show that the branches with $\Delta j = \pm 2$ and ± 4 are predominantly excited via resonances, while the branch with $\Delta j = 0$ contains a large contribution from direct scattering. The absolute rotational cross sections for $\Delta j = \pm 4$ are measured; they exhibit a large magnitude (10^{-16} cm^2) and peak and valley structures in the 1–4 eV range, reminiscent of well-known resonant vibrational excitation. The energy dependence and the absolute magnitude of the rotational cross sections for $\Delta j = \pm 4$ can be understood in terms of a "boomerang" calculation. A comparison of the experiment with the relevant theoretical calculations is made.

I. INTRODUCTION

Rotational and vibrational excitation are the major inelastic scattering processes in low-energy electron impact on molecules. In addition to a fundamental interest, these energy-loss mechanisms also play a dominant role in gas discharges.[1] Whereas there exist extensive measurements on vibrational cross sections,[2] the direct study of rotational cross sections have been confined[3,4] to H_2 and D_2 because of the high resolution required to resolve rotational transitions in most molecules.

In N_2, rotational cross sections at low electron energies have been theoretically studied by various approaches.[5-7] There seems to be a general agreement on the dominant role of the $^2\Pi_g$ shape resonance on rotational excitation in the energy range 1–4 eV with selection rules on rotational quantum number $\Delta j = 0$, ± 2, and ± 4. The magnitude of the calculated cross sections, however, strongly depends on the approach. The peak cross sections calculated for $j = 0 \rightarrow 4$ transition near 2.3 eV vary[6,7] from 2×10^{-15} to 3×10^{-17} cm^2.

We present in this paper a crossed-beam study of rotational excitation in N_2 with an apparatus resolution of 18 meV [full width at half-maximum (FWHM) of energy-loss peaks]. The absolute rotational-vibrational ($v = 0 \rightarrow 1$) cross sections are determined for the $\Delta j = \pm 4$ branches in the 1–4 eV range. As will be seen in Sec. III A, the present apparatus resolution is much larger than the energy spacing of adjacent rotational lines (1 meV for $\Delta j = 2$ and 2 meV for $\Delta j = 4$) but comparable to that of adjacent rotational branches (at 300 °K, 8.5 meV between $\Delta j = 0$ and $\Delta j = 2$; 19 meV between $\Delta j = 0$ and $\Delta j = 4$). For large values of j, the branches with $\Delta j = \pm 4$ are separable from the branches with $\Delta j = 0$ and ± 2. Hence, direct measurement of the energy dependence for $\Delta j = \pm 4$ is possible. The cross sections are made absolute with the help of the experimentally determined elastic and vibrational cross sections and the corresponding branching ratios. For the latter quantities, a numerical line-shape analysis is applied to the energy-loss profiles to extract the relative contribution of all rotational branches. While the branching ratios for the $v = 0 \rightarrow 1$ excitation have been theoretically studied by Read[8] and experimentally verified by Comer and Harrison,[9] the present approach using numerical analysis does not rely on the assumption of pure resonant scattering; hence, it is more general and is particularly applicable to the rotational excitation addressed in this work.

II. EXPERIMENT

A schematic diagram of the crossed-beam electron spectrometer is shown in Fig. 1. It is a modified version of the apparatus used by Boness and Schulz.[10] The operation and modifications[3] have been previously discussed, therefore only a brief description is given here.

The electron spectrometer consists of an electron monochromator, a molecular beam, and an electron-energy analyzer. Electrons emitted from a thoria-coated iridium filament are collimated and focused (electrodes A to $L1$) onto the entrance focal plane of the hemispherical analyzer of the monochromator. The energy-dispersed electron beam is refocused by this analyzer onto its exit focal plane. With proper adjustment of the exit

electron optics (electrodes $L2$ to $L3$), a monoenergetic electron beam with controlled energy is available to cross the molecular beam in the collision chamber. Electrons scattered within the acceptance angle of the analyzer electron optics (electrodes $L4$ to $L5$) are focused onto the entrance focal plane of the hemispherical analyzer, energy analyzed, and detected by the channeltron multiplier.

A constant energy resolution of 18 meV (FWHM of energy-loss peaks) is used for the present study. The apparatus profile is obtained from the electron scattering in Ar and is approximately a Gaussian. As a check on the Doppler broadening, we have also obtained energy-loss spectra in He whose mass is much smaller. Under similar experimental conditions, the apparatus profile obtained in He is practically identical to that of Ar in an energy range 0.5–5 eV and scattering angles 20°–110°. Hence, we conclude that the Doppler broadening is not significant in our crossed-beam studies. The introduction of N_2 into the scattering apparatus does not affect the profile. We note that the broadening of the elastic energy-loss peak due to rotational transition becomes negligibly small when the incident electron energy is less than 1 eV. In other words, the direct rotational excitation happens to be so small that the energy-loss profile obtained in N_2 is practically coincident with that in Ar. Based upon the above observations, we adopt the peak profile of Ar for all line-shape analysis discussed in Sec. III.

The energy scale is calibrated against the first peak, at 1.97 eV, in the vibrational excitation of N_2 to the $v=1$ level. The choice of 1.97 eV instead of an older value 1.93 eV is in view of a more accurate measurement of the energy position of the $^2\Pi_g$ resonance by Eyb[11] using the cusp structure of Na as reference. All absolute differential cross sections reported here are normalized to the elastic cross section of He with a procedure previously described.[3]

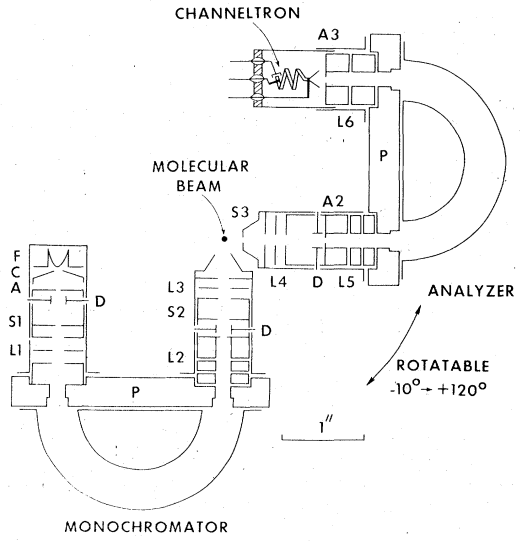

FIG. 1. Schematic diagram of the double electrostatic electron-impact spectrometer.

III. RESULTS

A. Energy-loss spectra and line-shape analysis

Figure 2 shows an energy-loss spectrum in N_2 obtained at an incident energy of 2.27 eV and at a scattering angle of 60°. The contribution of rotational transitions broaden the vibrational peak ($v=0\rightarrow 1$) by a factor of 2 and also the elastic peak profile in the wings. In both cases, the broadened profile lies within the expected range for the rotational branches $\Delta j=0$, ± 2, and ± 4 of N_2 molecules at a temperature of 300 °K. When the scattering angle is changed from 20° to 100°, the rotational broadening in the energy-loss peaks varies significantly.

In order to determine the branching ratios of the rotational transitions in the elastic and the vibrational peaks, a line-shape analysis is used. The analysis is a least-squares fit of the rotational branch profiles to a given energy-loss profile based on the following.

(i) The nitrogen molecules generated by the effusive molecular-beam source are in rotational equilibrium given by an initial population[12]

$$N(j)\sim g_I(2j+1)\exp[-B_e j(j+1)/kT], \qquad (1)$$

where $N(j)$ is the population of N_2 in rotational quantum number j. The nuclear-spin degeneracy factor $g_I=6$ for even j and $g_I=3$ for odd j. B_e

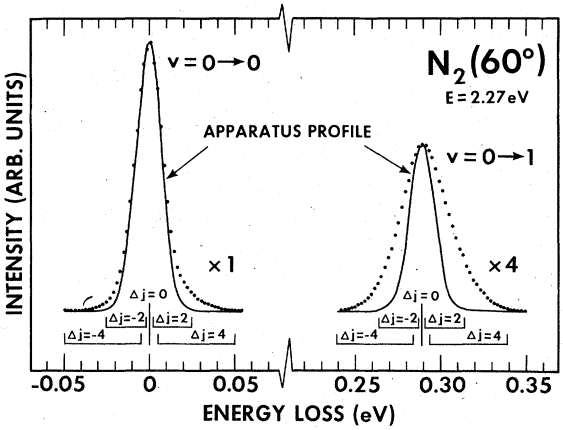

FIG. 2. Energy-loss spectrum of N_2 spanning the elastic and the $v=1$ region. The half-width of the apparatus profile is 18 meV. The expected ranges for the rotational branches $\Delta j=0$, ± 2 and ± 4 are indicated.

$= 0.25$ meV is the rotational constant of N_2 in its ground electronic and vibrational state. The temperature of the gas T is estimated to be 300 °K, the same as that of the nozzle of the molecular beam.

(ii) Only rotational transitions $\Delta j = 0, \pm 2$, and ± 4 are required to be considered in the data analysis. The exclusion of transitions with $\Delta j =$ (odd value) follows from the homonuclear nature of the N_2 molecule and the assumption that the nuclear spins are conserved in the collision. While the direct process is expected to contribute to $\Delta j = 0$ and ± 2, the existence of a strong $d\pi$ partial wave in the $^2\Pi_g$ resonance allows the maximum $\Delta j = l(d\pi) + l(d\pi) = 4$. Transitions with $|\Delta j| \geq 6$ are expected to be negligible.

(iii) The rotational-transition peak intensity profile is conveniently divided into five branches, characterized by $\Delta j = -4, -2, 0, +2$, and $+4$. The peak intensity profile of a given Δj branch is characterized by

$$\sum_{j=0}^{\infty} N(j)\sigma(j, \Delta j)\delta[E - B_e(2j + 1 + \Delta j)\Delta j], \qquad (2)$$

where j is the initial rotational quantum number and E is the energy of the scattered electrons. The argument in the δ function designates the energy position of the individual $j \rightarrow j + \Delta j$ rotational lines. The experimentally observed energy-loss profile is the sum of all branches given by Eq. (2) after convolution with the apparatus profile.

In N_2, the rotational constant $B_e = 0.25$ meV yields an adjacent rotational line spacing of $4B_e = 1$ meV for $\Delta j = \pm 2$ branches and $8B_e = 2$ meV for $\Delta j = \pm 4$ branches. At a temperature of 300 °K, states up to about $j = 22$ are involved in rotational transitions. Therefore, the energy ranges for $\Delta j = 2$ and $\Delta j = 4$ branches are 1.5–24 meV and 5.0–49 meV, respectively. In the present study, the apparatus profile has a Gaussian energy dependence with a half-width of 18 meV equally contributed by the monochromator and analyzer individually with a half-width of 12.7 meV. The energy-loss profile for the elastic and the vibrational peaks are analyzed in terms of five branches $\Delta j = 0, \pm 2, \pm 4$. For the present purposes, the branch profile given by Eq. (2) is further simplified with a continuous branch approximation proposed by Read.[8] Namely, the discrete initial population $N(j)$ is replaced by a continuous Boltzmann distribution neglecting the nuclear-spin statistics, and the rotational-transition cross section $\sigma(j, \Delta j)$ is assumed to be independent of the initial j value. The second assumption amounts to a high-j approximation[8] for the rotational transition. Since the average rotational quantum for N_2 at 300 °K is $j = 7$, the overall error introduced is expected to be small.

Figures 3(a) and 3(b) show the results of the line-

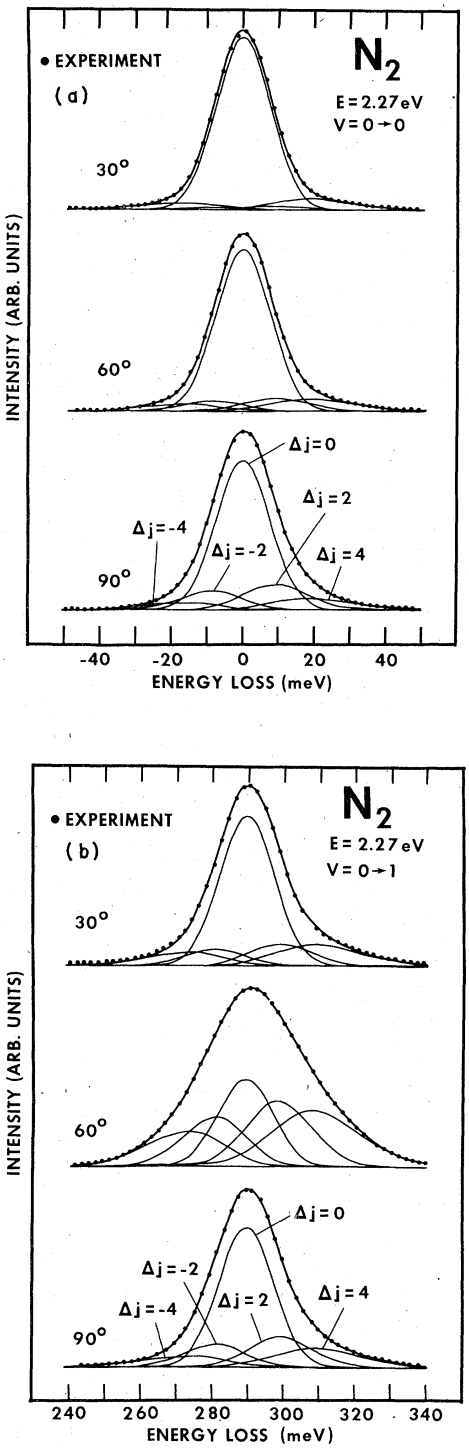

FIG. 3. (a) Line-shape analysis for the $v = 0 \rightarrow 0$ energy-loss profile. The area under each Δj branch profile gives the relative rotational cross section. The curve passing through the data points is the sum of all branch profiles. (b) Line-shape analysis for the $v = 0 \rightarrow 1$ energy-loss profile. The convention is the same as shown in Fig. 3(a).

shape analysis as applied to the energy-loss spectra at an incident energy of 2.27 eV and at scattering angles of 30°, 60°, and 90°. The solid curve that passes through each experimental energy-loss profile is the sum of the five lower curves which are the $\Delta j = 0, \pm 2, \pm 4$ branches convoluted with the apparatus profile. Despite the fact that there are five rotational branches, only the heights for $\Delta j = 0, 2, 4$ branches are adjusted to obtain agreement with the observed energy-loss profile. The heights for $\Delta j = -2$ and -4 branches are fixed by the corresponding $\Delta j = 2$ and 4 branches via detailed balancing.

The energy-loss profile for rotational branches $\Delta j = 0, \pm 2, \pm 4$ thus obtained from the line-shape analysis are then integrated under the individual curves to yield relative areas and hence the branching ratios for the rotational transitions. In light of Eq. (2), the branching ratios are the relative rotational and rotational-vibrational ($v = 0 \rightarrow 1$) cross sections, defined as $\sigma(\Delta j) \equiv \sum_j N(j)\sigma(j, \Delta j)$. The inclusion of the $\Delta j = \pm 6$ branch in the line-shape analysis yields a relative cross section two orders of magnitude lower than that for $\Delta j = 0, \pm 2, \pm 4$. We therefore consider the contribution of $\Delta j = \pm 6$ negligible.

B. Angular dependence of branching ratios

Figure 4 shows the angular dependence of the branching ratios of rotational-vibrational cross sections ($v = 0 \rightarrow 1$). The branching ratios are defined such that the sum over $\Delta j = 0, \pm 2$, and ± 4 is unity. The experimental data points are obtained from the line-shape analysis discussed in Sec. III A. The theoretical predictions involve the angular-distribution calculation applied to the resonant $d\pi$ partial waves and the rotational-impulse approximation for the $^2\Pi_g$ resonance. This approach has been used by Abram and Herzenberg,[13] and Chang and Temkin[14] on H_2 and by Read and Andrick[15] on a generalized formulation. The theoretical calculation relevant to the present studies is outlined in the Appendix.

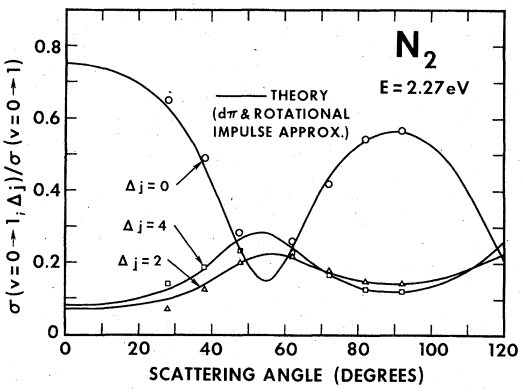

FIG. 4. Branching ratios of rotational-vibrational cross sections. The experimental data points are from the line-shape analysis at 2.27 eV. The theoretical results are based on the angular distributions given in Table I. The branching ratios for $\Delta j = -2$ and -4 are specified by detailed balancing to be 0.738 and 0.572 of that for $\Delta j = 2$ and 4, respectively.

It is seen from Fig. 4 that the theoretical branching ratio for $\Delta j = 0$ differs in major ways from those for $\Delta j = 2$ and 4. Whereas the branching ratio for $\Delta j = 0$ has maxima at 0° and 90° and a minimum near 55°, the trends for the branching ratios of $\Delta j = 2$ and 4 are just the opposite. There is also a reversal of the dominance in magnitude between the branching ratios of $\Delta j = 2$ and 4 at scattering angles below and above 70°. These predictions are in good agreement with the experimental results over scattering angles 30°–90°. The present findings are consistent with the previous observations of rotational broadening in the $v = 0 \rightarrow 1$ energy-loss peak by Comer and Harrison.[9] For application purposes, Table I lists the angular dependence of the rotational transitions and their angle-integrated branching ratios as calculated for the $^2\Pi_g$ resonance.

For pure rotational cross sections, the branching ratios from line-shape analysis significantly differ from those for vibrational cross sections as shown in Figs. 3(a) and 3(b). This is not unexpected because of the possibility of large contribution to $\Delta j = 0$ via direct scattering. Hence, the angular

TABLE I. High-j approximation of the relative rotational cross sections via $^2\Pi_g$ resonance. $d\sigma(\theta, \Delta_j)/d\Omega$ equals the product of the relative amplitude and the angular distribution (normalized to 4π). It should be noted that

$$\frac{d\sigma(\theta)}{d\Omega} \equiv \sum_{\Delta j} \frac{d\sigma(\theta, \Delta j)}{d\Omega} = 1 \times \tfrac{15}{14}(1 - 3\cos^2\theta + \tfrac{14}{3}\cos^4\theta)$$

is the angular dependence of resonant vibrational excitation without the resolution of rotational transitions. The relative amplitudes given here are presented as the branching ratios of the angle-integrated rotational cross sections for $\Delta j = 0$, ± 2, and ± 4. The angular distributions for different Δj's are obtained with Eqs. (A4) and (A5) using $l = 2$ and $m = \pm 1$. They are in agreement with a more general approach used by Read.[8]

Rotational transitions	$\frac{d\sigma}{d\Omega}(\theta, \Delta j)$
$\Delta j = -4$	$0.091 \times \frac{45}{56}(1 + \frac{2}{3}\cos^2\theta + \frac{1}{9}\cos^4\theta)$
-2	$0.106 \times \frac{15}{14}(1 - \cos^2\theta + \frac{4}{3}\cos^4\theta)$
0	$0.500 \times \frac{135}{112}(1 - \frac{46}{9}\cos^2\theta + \frac{23}{3}\cos^4\theta)$
+2	$0.144 \times \frac{15}{14}(1 - \cos^2\theta + \frac{4}{3}\cos^4\theta)$
+4	$0.159 \times \frac{45}{56}(1 + \frac{2}{3}\cos^2\theta + \frac{1}{9}\cos^4\theta)$

correlation calculation based on $d\pi$ partial waves is not applicable here. In order to study the role of resonant contribution to rotational transitions, we measured the angular dependence of the elastic cross sections containing all rotational contributions in addition to the branching ratios. The product of these two quantities yield the rotational-branch cross sections. Within an experimental uncertainty of about 25%, the angular dependence for $\Delta j = \pm 4$ and ± 2 over scattering angles 30° to 90° is consistent with the resonant prediction listed in Table I, but not with that for $\Delta j = 0$.

C. Energy dependence and absolute cross sections

The results of line-shape analysis in Figs. 3(a) and 3(b) suggest that the signals in both the elastic and vibrational peaks are dominated by the $\Delta j = \pm 4$ transitions, when the energy-loss is more than 30-meV off center. Hence, the energy dependence of these wings is just the energy dependence of $\sigma(\Delta j = \pm 4)$, providing that $\sigma(j; \Delta j)$ is insensitive to j. As a test, we have measured the energy dependence of rotational and rotational-vibrational transitions at energy losses of 30, 40, and 50 meV off the center peak in the energy range 1–4 eV. All three energy dependences of each transition agree with one another to within experimental error of about 1%. In other words, $\sigma(j; \Delta j)$ is insensitive to j in the range $j = 12$–20 for $\Delta j = \pm 4$. The present apparatus resolution, however, does not enable us to directly study the energy dependence for $\Delta j = 0$ and ± 2 transitions.

Figure 5 shows the energy dependence of the differential rotational and rotational-vibrational cross sections for $\Delta j = \pm 4$ at 60° scattering in the energy range 1–4 eV. The temperature of N_2 is estimated to be 300 °K which yields an average rotational quantum of $j = 7$. The dominance of the $^2\Pi_g$ resonant contribution to these cross sections is exhibited in the fine structure in their energy dependence, with the profile peaked near 2.3 eV. For rotational excitation, the energies of the resonant peaks are lower than those of the rotational-vibrational excitation and the excitation profile is also broader.

The absolute magnitudes of the cross sections shown in Fig. 5 are obtained from the rotationally summed elastic and vibrational cross sections at 2.27 eV and the corresponding branching ratios. Since the excitation here is characterized by a single $d\pi$ partial wave, the *energy dependence is independent of scattering angles*. Total cross sections can be obtained from differential cross sections at 60° by integrating the angular distribution for $\Delta j = 4$ given in Table I. This procedure amounts to multiplying the differential cross sections given in Fig. 5 by $1.06 \times 4\pi$. This yields a maximum rotational cross section, at 2.21 eV, of $(2.1 \pm 0.8) \times 10^{-16}$ cm^2 and a maximum rotational-vibrational ($v = 0 \rightarrow 1$) cross section, at 2.27 eV, of $(0.90 \pm 0.3) \times 10^{-16}$ cm^2.

The differential rotational and rotational-vibrational cross sections for $\Delta j = -4$ are observed to have similar energy dependence to those for $\Delta j = +4$. The absolute magnitude of cross sections can be determined with the branching ratios given in Table I.

A comparison of the absolute vibrational cross section ($v = 0 \rightarrow 1$) in the energy range 1–4 eV between our experiment and the absolute boomerang theory has been given by Dubé and Herzenberg.[16] The agreement on both resonant structures and absolute magnitudes over the whole range is within 10%. The angular dependence of the branching ratios given in Fig. 4 provides further support of the view of resonant excitation.

Figure 6 presents a comparison of the differential rotational cross section for $\Delta j = 4$ between experiment and a boomerang calculation. The shift of energies in the resonant peaks of the rotational cross sections is also accounted for by the theory. The agreement on the energy dependence of the absolute cross sections is good except at energies larger than 3 eV. The experimental cross section decreases less rapidly with increasing energy than that calculated by the boomerang theory.

A *direct comparison* of the experiment with other theoretical calculations is difficult due to the limi-

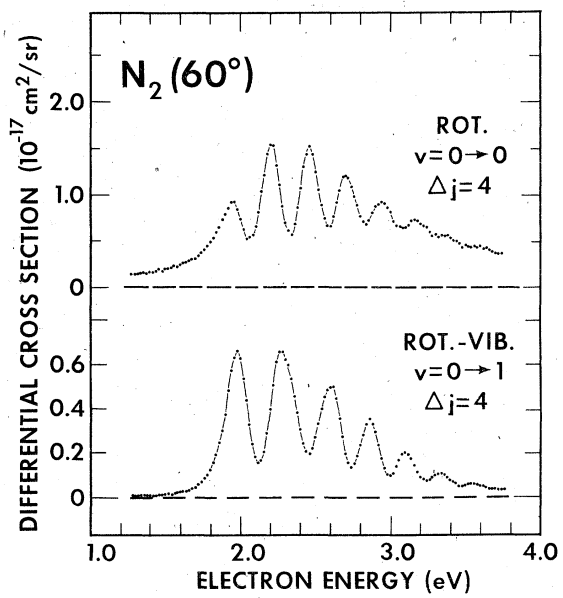

FIG. 5. Energy dependence of rotational and rotational-vibrational cross sections for $\Delta j = 4$. The experimental errors in the cross sections are about 35% and 25%, respectively.

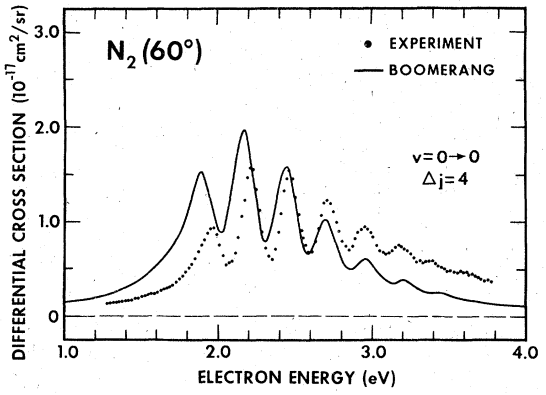

FIG. 6. Comparison of the absolute differential rotational cross sections for $\Delta j = 4$ in N_2 as a function of electron energy. The errors in the *absolute magnitude* of experimental cross sections are about 35%. The theoretical calculation is based on the absolute boomerang theory of Dubé and Herzenberg on vibrational excitation, as discussed in Sec. III C.

tation of the published information. In the hybrid calculation of Chandra and Temkin[5] and the resonant calculation of Chen,[7] only the low-j transition with initial $j = 0$ and 1 are presented. Nevertheless the dependence of rotational cross sections on the initial j values has been studied by Chandra and Burke.[6] Their results suggest that the rotational cross section for $\Delta j = 4$ at $T = 300\,^{\circ}\mathrm{K}$ is one-third of that for $j = 0 \rightarrow 4$ transition and one-half of that for $1 \rightarrow 5$ transition. Under this assumption, we find our results for $\Delta j = 4$ are consistent with the hybrid calculations in the absolute magnitude of the peak cross sections and the general profile of the energy dependence. But the detailed resonance structures, such as the number and energy spacing of resonant peaks, are not accounted for by this calculation.

IV. DISCUSSION

In this paper the rotational and rotational-vibrational excitation in N_2 have been studied with a crossed-beam method in the range of 1–4 eV. Rotational transitions with $\Delta j = \pm 4$ as well as those with $\Delta j = \pm 2$ are strongly observed. The excitation of the rotational branch $\Delta j = \pm 4$ can be understood in terms of the incoming and outgoing resonant $d\pi$ partial waves, each of which carries two units of angular momentum for exchange with those in the nuclear motion. The observed angular and energy dependences of the differential cross sections lend support to this view. For pure rotational excitation, the resonant structures in the energy dependence are shifted down below that of rotational-vibrational excitation to $v = 1$. The general features and the peak rotational cross sections of $(2.1 \pm 0.8) \times 10^{-16}$ cm^2 for $\Delta j = 4$ are in good agreement with an absolute boomerang calculation previously used by Dubé and Herzenberg.[16] The peak rotational cross sections can also be accounted for by the hybrid calculations of Chandra and Temkin[5] on $j = 0 \rightarrow 4$ and $j = 1 \rightarrow 5$ transitions extrapolating the j dependence given by Chandra and Burke.[6]

ACKNOWLEDGMENTS

We wish to acknowledge the late G. J. Schulz for his assistance and encouragement that made this work possible. We also wish to thank A. V. Phelps for his continued interest in and comments on this work. Thanks go to A. Herzenberg, A. Temkin, and I. C. Walker for their valuable suggestions, and to J. M. Phillips, M. Allen, and J. Kearney for their general assistance. Finally, we thank F. H. Read for his helpful comments on the manuscript. This work was supported by the Office of Naval Research.

APPENDIX

In the rotational impulse approximation, the scattering amplitude $f(\underline{k}_i, \underline{k}_f)$ for a rotation transition $J_i M_i \rightarrow J_f M_f$ involving Σ electronic states is given by[13,14]

$$f(\underline{k}_i, \underline{k}_f) = \int Y^*_{J_f M_f}(\hat{\underline{R}})\, f(\underline{k}_i, \underline{k}_f; \hat{\underline{R}})\, Y_{J_i M_i}(\hat{\underline{R}})\, d\hat{\underline{R}}, \quad \text{(A1)}$$

where $f(\underline{k}_i, \underline{k}_f; \hat{\underline{R}})$ is the scattering amplitude for a molecule having the fixed orientation $\hat{\underline{R}}$. For purely resonant process, this fixed-axis scattering amplitude between specific vibrational states v_i and v_f of the target molecule may be derived as[17]

$$f(\underline{k}_i, \underline{k}_f; \hat{\underline{R}}) = 16\pi^3 \rho(v_i, v_f; E) \sum_m Y_{l_f m}(\hat{\underline{k}}'_f)\, Y^*_{l_i m}(\hat{\underline{k}}'_i), \quad \text{(A2)}$$

with $\rho(v_i, v_f; E)$ representing an energy term that depends on the details of the radial wave function of the compound state, as well as on the initial and final vibrational wave functions. E is the incident electron energy, l_f and l_i are the incoming and outgoing partial waves, respectively, and the prime in the wave vectors indicates that they are defined with respect to the body-fixed frame. Equation (A2) contains implicitly the approximation that the scattering is due to only one partial wave in the in- and out-channel: For $^2\Pi_g$ resonance in N_2, $l_i = l_f = 2$ and $m = \pm 1$.

Using (A2) in (A1), the differential cross section is obtained by summing over unobserved final M_f and averaging over M_i:

$$\frac{d\sigma}{d\Omega}(v_i J_i \rightarrow v_f J_f) = \frac{k_f}{k_i} \frac{1}{2J_i + 1} \sum_{M_i, M_f} |f(\underline{k}_i, \underline{k}_f)|^2 \quad \text{(A3)}$$

with

$$k_f^2 = k_i^2 + 2\{\omega(v_i - v_f) + (1/2I)[J_i(J_i + 1) - J_f(J_f + 1)]\}.$$

Making use of the high-J approximation,[8] we obtain an expression for the differential cross section for excitation in the ΔJ branch,

$$\frac{d\sigma}{d\Omega}(v_i \to v_f, \Delta J) = \frac{k_f}{k_i} |\rho(v_i, v_f; E)|^2 16\pi^4 \times \sum_L A_L(\Delta J) P_L(\cos\theta), \quad \text{(A4)}$$

where

$$A_L(\Delta J) = (-)^L (2L+1)(2l_i+1)(2l_f+1) \times \begin{pmatrix} l_i & l_i & L \\ 0 & 0 & 0 \end{pmatrix} \begin{pmatrix} l_f & l_f & L \\ 0 & 0 & 0 \end{pmatrix} \times \sum_j (-)^j (2j+1) [d^j_{0,\Delta J}(\tfrac{1}{2}\pi)]^2 \times \begin{Bmatrix} l_i & l_i & L \\ l_f & l_f & j \end{Bmatrix} \left[\sum_m (-)^m \begin{pmatrix} l_i & l_f & j \\ m & -m & 0 \end{pmatrix} \right]^2, \quad \text{(A5)}$$

and $d^j_{0,\Delta J}(\theta)$ are the reduced rotation matrices.[18]

The angular terms in (A4) are consistent with the earlier work of Read.[8] The simplicity of the expressions for A_L given in (A5) is due to the explicit use of single partial waves in the scattering formalism. Note further that if one neglects the energy loss due to rotational transitions, we have the relation

$$\sum_{\Delta J} \frac{d\sigma}{d\Omega}(v_i \to v_f; \Delta J) \simeq \frac{d\sigma}{d\Omega}(v_i \to v_f). \quad \text{(A6)}$$

This last expression provides the connection between the individual rotational-vibrational branch and the vibrational cross sections. The present formalism together with the boomerang treatment for energy dependence[16] yields the *absolute* rotational cross section shown in Fig. 6.

[1] A. V. Phelps, Rev. Mod. Phys. 40, 399 (1968).

[2] For a review, see G. J. Schulz, *Principles of Laser Plasmas*, edited by G. Bekefi (Interscience, New York, 1976), Chap. 2; a compilation of cross sections has been given by L. J. Kieffer, Joint Institute for Laboratory Astro-physics, Report No. 13, 1973 (unpublished).

[3] H. Ehrhardt and F. Linder, Phys. Rev. Lett. 21, 419 (1968); F. Linder and H. Schmidt, Z. Naturforsch. A 26, 1603 (1971); G. Joyez, J. Comer, and F. H. Read, J. Phys. B 6, 2427 (1973); S. F. Wong and G. J. Schulz, Phys. Rev. Lett. 32, 1089 (1974); S. K. Srivastava, R. I. Hall, S. Trajmar, and A. Chutjian, Phys. Rev. A 12, 1399 (1975); J. F. Williams, *Ninth International Conference on the Physics of Electronic and Atomic Collisions: Abstracts of Papers*, edited by J. S. Risley and R. Geballe (University of Washington, Seattle, 1975), p. 265.

[4] E. S. Chang and S. F. Wong, Phys. Rev. Lett. 38, 1327 (1977).

[5] N. Chandra and A. Temkin, Phys. Rev. A 14, 507 (1976).

[6] N. Chandra and P. G. Burke, J. Phys. B 6, 2355 (1973).

[7] J. C. Y. Chen, Phys. Rev. 146, 61 (1966), and references therein.

[8] F. H. Read, J. Phys. B 5, 255 (1972).

[9] J. Comer and M. Harrison, J. Phys. B 6, L70 (1973).

[10] M. J. W. Boness and G. J. Schulz, Phys. Rev. A 9, 1969 (1974).

[11] M. Eyb, Ph.D. thesis (University of Kaiserslautern, 1974) (unpublished). A recent recalibration using the cusp feature in HF has also been made by K. Rohr [J. Phys. B 10, 2215 (1977)]. We here calibrate the first resonant peak observed in the $v = 0 \to 1$ excitation with respect to the elastic features reported in their work. The uncertainty of the present energy scale is 30 meV.

[12] G. Herzberg, *Spectra of Diatomic Molecules* (Van Nostrand, New York, 1950).

[13] R. A. Abram and A. Herzenberg, Chem. Phys. Lett. 3, 187 (1969).

[14] E. S. Chang and A. Temkin, Phys. Rev. Lett. 23, 399 (1969).

[15] F. H. Read and D. A. Andrick, J. Phys. B 4, 911 (1971).

[16] L. Dubé and A. Herzenberg, *Ninth International Conference on the Physics of Electronic and Atomic Collisions: Abstracts of Papers*, edited by J. S. Risley and R. Geballe (University of Washington, Seattle, 1975), p. 264.

[17] D. T. Birtwistle and A. Herzenberg, J. Phys. B 4, 53 (1971).

[18] D. M. Brink and G. R. Satchler, *Angular Momentum*, 2nd ed. (Clarendon, Oxford, 1968).